

N. A. Dunn, J. S. Conery and S. R. Lockery

J Neurophysiol 98:888-897, 2007. First published May 23, 2007; doi:10.1152/jn.00074.2007

You might find this additional information useful...

This article cites 45 articles, 18 of which you can access free at:

<http://jn.physiology.org/cgi/content/full/98/2/888#BIBL>

Updated information and services including high-resolution figures, can be found at:

<http://jn.physiology.org/cgi/content/full/98/2/888>

Additional material and information about *Journal of Neurophysiology* can be found at:

<http://www.the-aps.org/publications/jn>

This information is current as of December 27, 2007 .

Circuit Motifs for Spatial Orientation Behaviors Identified by Neural Network Optimization

N. A. Dunn,¹ J. S. Conery,² and S. R. Lockery¹

¹Institute of Neuroscience and ²Department of Computer Science, University of Oregon, Eugene, Oregon

Submitted 22 January 2007; accepted in final form 18 May 2007

Dunn NA, Conery JS, Lockery SR. Circuit motifs for spatial orientation behaviors identified by neural network optimization. *J Neurophysiol* 98: 888–897, 2007. First published May 23, 2007; doi:10.1152/jn.00074.2007. Spatial orientation behavior is universal among animals, but its neuronal basis is poorly understood. The main objective of the present study was to identify candidate patterns of neuronal connectivity (motifs) for two widely recognized classes of spatial orientation behaviors: hill climbing, in which the organism seeks the highest point in a spatial gradient, and goal seeking, in which the organism seeks an intermediate point in the gradient. Focusing on simple networks of graded processing neurons characteristic of *Caenorhabditis elegans* and other nematodes, we used an unbiased optimization algorithm to seek values of neuronal time constants, resting potentials, and synaptic strengths sufficient for each type of behavior. We found many different hill-climbing and goal-seeking networks that performed equally well in the two tasks. Surprisingly, however, each hill-climbing network represented one of just three fundamental circuit motifs, and each goal-seeking network comprised two of these motifs acting in concert. These motifs are likely to inform the search for the real circuits that underlie these behaviors in nematodes and other organisms.

INTRODUCTION

Spatial orientation behavior is universal among animals but its neuronal basis is poorly understood. The nematode *Caenorhabditis elegans* is an effective model system for studies of spatial orientation in two main respects. First, it expresses a diverse repertoire of orientation behaviors including chemotaxis to soluble (Ward 1973) and volatile compounds (Bargmann and Horvitz 1991), thermal migration and isothermal tracking (Hedgecock and Russell 1975), aerotaxis (Chang et al. 2006; Cheung et al. 2005), avoidance of high osmolarity (Culotti and Russell 1978) and toxins (Sambongi et al. 1999), and localization of food patches (Tsalik and Hobert 2003). Second, *C. elegans* offers several unusual experimental advantages including a compact nervous system of only 302 neurons, a nearly complete anatomical wiring diagram, and a wide range of genetic and physiological techniques for linking genes and molecules to behavior. Nevertheless, the elucidation of the neuronal basis of *C. elegans* spatial orientation behaviors is at an early stage. To facilitate these studies, we have taken a theoretical approach in which we have attempted to identify minimal patterns of neuronal connectivity, which we refer to as “motifs” (Milo et al. 2002), that are sufficient to produce oriented behavior in realistic environments.

Each of the most frequently studied forms of spatial orientation in *C. elegans* falls into one of two broad classes. The first

class, represented by the two forms of chemotaxis, is hill climbing, in which the animal endeavors to reach the highest point in the concentration gradient. The second class, represented by thermotaxis and aerotaxis, is goal seeking, in which the animal seeks an intermediate location in the gradient. In thermotaxis, this location is the animal’s preferred temperature, usually the temperature at which it has found food in the past (Hedgecock and Russell 1975); in aerotaxis, this location is its preferred oxygen concentration (5–11%), which, like preferred temperature, can be modified by experience (Cheung et al. 2005; Gray et al. 2004).

This paper asks the question of whether hill-climbing and goal-seeking behaviors in *C. elegans* might be served by similar motifs. To address this question, we modeled *C. elegans* neurons as passive, isopotential nodes with simple first-order dynamics (single time constants) and graded synaptic transmission. These assumptions are broadly consistent with preliminary electrophysiological recordings and calcium imaging experiments in *C. elegans* (Goodman et al. 1998; Suzuki et al. 2003) and are amenable to a well-studied class of differential equations (Beer 1995, 2006). Time constants, resting potentials (biases), and the signs and strengths of synaptic connections were adjusted by simulated annealing, a parameter optimization algorithm in which model networks propagate themselves across virtual generations with only the fittest network surviving to reproduce. Fitness was defined in terms of spatial orientation ability. A key aspect of the design of this study was to vary the nature of the spatial orientation task—hill climbing versus goal seeking—while keeping all other aspects of the simulation fixed including gradient steepness, network architecture, and motor representation. This design enabled us to attribute changes in time constants, biases, and connectivity to changes in task.

We found that hill-climbing and goal-seeking behavior in our models were subserved by three fundamental motifs. The main difference between the networks optimized for the two behaviors was that hill-climbing networks relied on a single motif, whereas goal-seeking networks relied on two distinct motifs, one that was active below the goal and one that was active above the goal. We conclude that hill-climbing and goal-seeking behavior in *C. elegans* may involve similar motifs. These motifs provide testable hypotheses as to the neuronal basis of spatial orientation behaviors in this and other systems.

METHODS

To identify minimal networks for hill-climbing and goal-seeking behavior, we used an optimization algorithm to adjust key parameters in an idealized model that captured the essential aspects of spatial orientation behaviors and their neuronal basis in *C. elegans*. Accord-

Address for reprint requests and other correspondence: S. Lockery, Institute of Neuroscience, 1254 University of Oregon, Eugene, OR 97403 (E-mail: shawn@lox.uoregon.edu).

ingly, the model was constrained by three main assumptions: 1) detection of sensory input at a single point in space is sufficient for hill-climbing and goal-seeking behaviors in *C. elegans*. 2) Hill climbing and goal seeking share a common behavioral mechanism, namely the modulation of turning frequency as a function of sensory input. And 3) the *C. elegans* nervous system functions mainly as a network of graded (analog) processing elements.

Assumption 1 reflects the anatomy and distribution of sensory organs in *C. elegans* (Bargmann and Horvitz 1991; Ward 1978; Ward et al. 1975). *Assumption 2* reflects the findings of behavioral analyses of turning frequency during orientation behaviors (Chung et al. 2006; Dusenbery 1980; Miller et al. 2005; Ryu and Samuel 2002; Zariwala et al. 2003). *Assumption 3* reflects the apparent absence of all-or-none action potentials in *C. elegans* and other nematodes (Davis and Stretton 1989; Goodman et al. 1998).

Model networks

Model networks had the same initial architecture regardless of the nature of the spatial orientation task (Fig. 1). This architecture had three main features.

SMALL NUMBER OF SENSORY NEURONS AND INTERNEURONS. The maximum number of sensory neurons was two, reflecting that fact that in pilot studies we were unable to optimize networks to perform goal-seeking behavior with a single sensory neuron. This result is consistent with the suggestion, based on indirect experimental evidence (Mori and Ohshima 1995), that *C. elegans* thermotaxis, an example of goal-seeking behavior, involves at least two thermosensory neurons. The maximum number of interneurons was one. This was done to encourage minimal solutions and to simplify post hoc analysis of network function. On some trials, the optimization algorithm found solutions using the maximum number of neurons, whereas on other trials, it found solutions involving fewer neurons.

STOCHASTIC OUTPUT NEURON. The most frequent type of direction change in *C. elegans* spatial orientation behaviors is a so-called reversal in which an animal that is moving forward backs up momentarily, then resumes forward movement in a new direction (Gray et al. 2005). Reversals occur stochastically with an average frequency that is regulated by a network of command interneurons for forward and

reverse locomotion (Chalfie et al. 1985; Zheng et al. 1999). Because the functional details of this network are unclear, the command network was represented by a single stochastic output unit that closely resembled a Boltzman or Hopfield neuron (Hopfield 1982).

FEEDFORWARD CONNECTIVITY. Feedback connections from the output node and from the interneuron were not allowed. This restriction was consistent with our goal of finding minimal patterns of synaptic connectivity rather than an exhaustive set of motifs. In previous work, we have documented the hill-climbing solutions that arise when this restriction is relaxed (Dunn et al. 2004). That study found that the main function of feedback connections was to reduce the effective time constants of the nodes in the network, rather than to contribute to neuronal computations underlying spatial orientation behavior per se.

Model neurons

The main aspects of the mathematical approach used here have been described previously (Dunn et al. 2004). Briefly, sensory neurons and interneurons were represented as passive, isopotential nodes according to the equation

$$\tau_i \frac{dA_i(t)}{dt} = -A_i(t) + \sigma(I_i) \tag{1}$$

where τ_i is the neuronal time constant, A_i is the activation level of neuron i in the network ($0 \leq A_i \leq 1$), I_i is the sum of inputs to neuron i , and $\sigma(I_i)$ is the sigmoidal logistic function $1/[1 + \exp(-I_i)]$. The time constant τ_i determined how rapidly activation approached its steady-state value for constant I_i .

Input I_i was equal to the sum of sensory and synaptic inputs to neuron i such that

$$I_i = \sum_j [w_{ji}A_j(t)] + b_i + w_{ui}u(t) \tag{2}$$

where w_{ji} is the synaptic weight from neuron j to neuron i , b_i is a bias term, $u(t)$ is sensory input, and w_{ui} is sensory input gain factor for neuron i . Self-connections w_{ii} represented the effects of either polysynaptic feedback or voltage-dependent currents (but not autapses). Allowing the optimization algorithm to incorporate such connections, if it so desired, was justified by anatomical reconstructions that demonstrate the possibility of polysynaptic feedback (White et al. 1986) and by electrophysiological recordings indicating the presence of voltage-dependent currents in *C. elegans* neurons (Goodman et al. 1998). The purpose of the gain factor was to adjust sensitivity to changes in the sensory gradient; w_{ui} was zero for nonsensory neurons.

The output unit, called *neuron 3* in Fig. 1, was a binary stochastic element. Its on state ($A_3 = 1$), was defined as continuous forward locomotion, henceforth a “run,” whereas its off state ($A_3 = 0$) was defined as a turn. At each time step in the simulation, the state of the output unit was updated probabilistically according to the equation

$$P_{\text{run}}(t) = \sigma[kI_3(t)] \tag{3}$$

where P_{run} is the probability of adopting the on-state and I_3 is the net input to the output unit given as $I_3(t) = \sum_j w_{j3}A_j(t)$. The quantity k determined the sensitivity of the unit to small changes in its input. We found that very small and very large values of k strongly affected the speed and success rate of the optimization algorithm. We selected an intermediate value of $k = 30$ by trial and error. Note that $P_{\text{turn}}(t) = 1 - P_{\text{run}}(t)$.

Simulation of behavior

A worm was represented as a point with a velocity in the x, y plane. Speed during forward locomotion was 0.15 mm/s; speed during turns

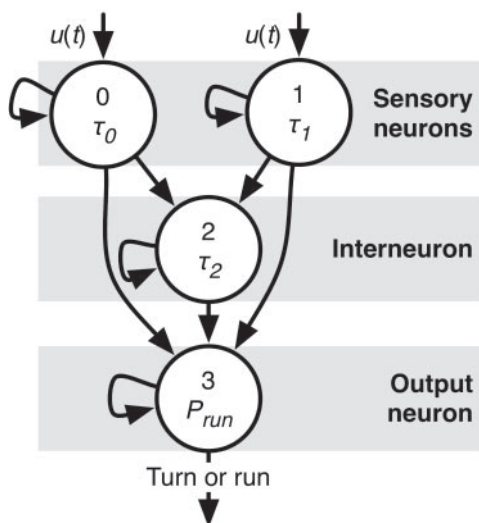


FIG. 1. The network model. Circles and arrows denote neurons and synaptic pathways, respectively. Neurons are numbered 0 through 3; neurons 0–2, were assigned unique time constants (τ) and biases (not shown). The state variable of neuron 3 was the probability of executing run behavior. The quantity $u(t)$ is sensory input, determined according to the location along the x axis as shown in Fig. 2.

was 0.11 mm/s (Dunn et al. 2004). Turns were modeled by sampling randomly from a uniform distribution of direction changes that exceeded a magnitude of 50°/s (Pierce-Shimomura et al. 1999). Model worms explored a virtual arena with a width of 30 cm (x axis), but with no limitations on the y axis (Fig. 2). Sensory input was a function of displacement along the x axis. In hill-climbing simulations, sensory input (in arbitrary units) varied linearly from a value of -2.5 at the extremes of the x axis to 0.5 at its center. In goal-seeking simulations, sensory input varied linearly from -2.5 to 3.5 such that the value at the center of the x axis and the gradient slope were the same as in hill-climbing simulations. Each model worm was simulated for 20 min; time-dependent quantities were updated at 1-s intervals.

Optimization of networks

Time constants, synaptic weights, and biases were optimized by simulated annealing. In hill-climbing simulations, networks were optimized to find the sensory maximum; in goal-seeking simulations, networks were optimized to find the location in the gradient where sensory input was 0.5 . To facilitate optimization, connection strengths and biases were restricted to the range -30 to $+30$, and time constants were restricted to the range $+3$ to $+30$. In accordance with standard simulated annealing procedures (Masters 1993; Press et al. 1992), the search radius was reduced exponentially in 500 so-called temperature steps; at each temperature, 200 parameter sets were evaluated. Thus an individual optimization run involved testing the orientation performance of 100,000 different parameter sets. Network performance (fitness), was quantified as the average distance (cm) of the model worm from its target location during a 20-min simulation. In pilot simulations, visual inspection of spatial trajectories showed that a fitness of 1.25 cm represented a well-functioning network. Parameter sets with a fitness at or above this value were taken as solutions; parameter sets with a fitness below this value were discarded. Simulations were distributed over an IBM p690 16-node, shared-memory server or an 11-node, Beowulf cluster. Software was written in C++ using MPI for parallelization, and the *Blitz++* library was used for array processing. Each optimization run took ~ 5 h to complete on either computer system.

Generalization tests

A key test of an optimized network is whether it responds correctly to inputs that were not presented during optimization. In the present study, generalization tests were important to ensure that an apparent

solution was not an accident of the gradient shape used during optimization or the initial states of the model neurons. Because optimization was performed in the context of planar gradients, the generalization tests were performed in radially symmetric gradients. Accordingly, sensory input varied linearly with radius, but different radial gradients were used for the two optimization tasks. Hill-climbing networks were tested in radial gradients imposed on a circular arena (4.5 cm in radius) such that the maximum sensory input (0.5) occurred at a radius of 2.5 cm. At the center and edge of the arena, sensory input was 0 and -0.125 , respectively. Goal-seeking networks were tested on conical gradients of two complementary types. In the first type, sensory input varied from -0.125 at the edge to a maximum (1.0) at the center; in the second type, input varied from a maximum (1.125) at the edge to a minimum (0.0) in the center. A solution was considered to generalize successfully if it reached the target location (sensory input = 0.5) in the generalization gradient 80% of the time (10 to 50 trials). Solutions that failed the generalization test were discarded, although this seldom occurred.

Motif identification

Solutions were classified initially by hand according to three distinct assessments of neuronal function. 1) The center and width of the range of sensory input over which neurons 0, 1, and 2 were neither in cut-off [$A_i(t) < 0.01$] nor saturation [$A_i(t) > 0.99$] during generalization tests. 2) The amplitude of empirically defined relaxation time constants of neurons 0, 1, and 2 were measured using white-noise stimulation of sensory neurons. Within each network, time constants were ranked on the basis of relative amplitude. 3) The respective signs of the two synaptic pathways from sensory input to the output neuron. For example, a pathway with two inhibitory synapses in series was scored as excitatory.

Manual classifications were confirmed by a subsequent cluster analysis defined over the three parameters generated by assessments 1 and 2 above. Hill-climbing networks fell into three classes (motifs) according to this analysis. Goal-seeking networks were more challenging to classify, but when the analysis was carried out separately for episodes in which the model worm was above or below the target, the three hill-climbing motifs could be recognized as described in the following text.

RESULTS

To identify motifs for spatial orientation behavior in *C. elegans*, we optimized networks to reach the target location in two distinct tasks: the hill-climbing task in which the target was the maximum level of sensory input in the gradient and the goal-seeking task in which the target was an intermediate level of sensory input. The present analysis concerns 50 hill-climbing solutions obtained from 50 optimization runs and 59 goal-seeking solutions obtained from 528 optimization runs (supporting Table 1¹).

Hill climbing

We found three different motifs sufficient for hill-climbing behavior. Two motifs involved networks that computed an approximation to the temporal derivative of sensory input; we refer to these as the interneuron differentiator and the sensory neuron differentiator motifs. We found 12 interneuron differentiator networks and nine sensory neuron differentiator networks. The third type of network used an altogether different

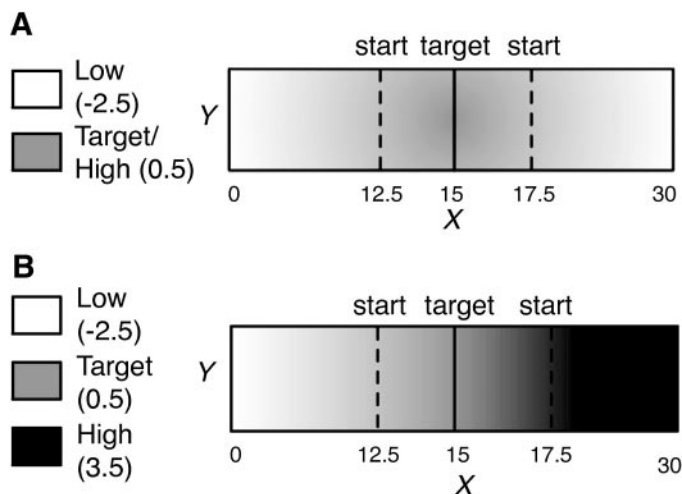


FIG. 2. Sensory input vs. spatial location in virtual arenas. A: hill-climbing arena. B: goal-seeking arena. Gray levels indicate the relative amplitude of sensory input as shown in the keys. Dimensions are in centimeters.

¹The online version of this article contains supplemental data.

strategy, which we refer to as the bounce-and-trap motif; we found 29 bounce-and-trap networks.

Interneuron differentiator motif

An example of this motif is shown in Fig. 3. The interneuron differentiator relied on a fast, excitatory pathway (*neuron 1* to *neuron 3*) in parallel with a slow, inhibitory pathway through the interneuron (*neuron 1* to *neuron 2* to *neuron 3*). The hill-climbing behavior of the network is shown in Fig. 3*B*, and the time course of neuronal activation is shown in *C*. The reduced speed of the slow inhibitory pathway was mainly the result of the comparatively large time constant on the interneuron relative to the sensory neuron. Turning events (labeled

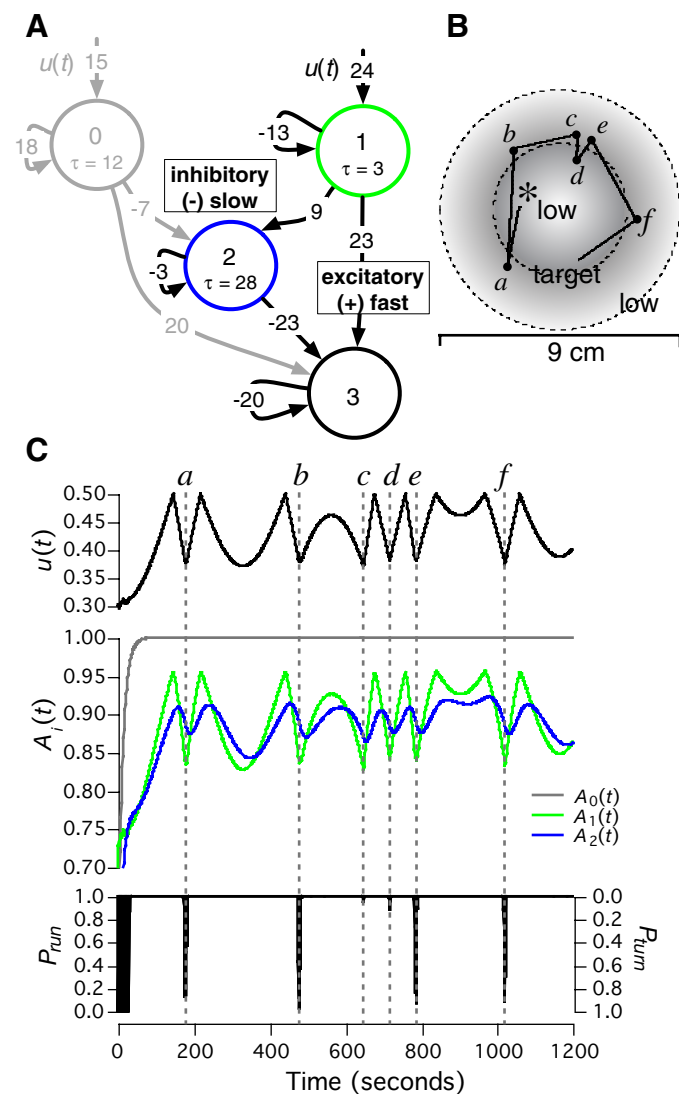


FIG. 3. Example of the interneuron differentiator motif. *A*: circuit diagram. Numbers associated with arrows indicate the strengths of synaptic connections or the sensory gain factor. Time constants are given in seconds. The biases of *neurons 1* and *2* were 3. *Neuron 0*, shown in gray, was excluded from the motif because its activation level was constant during hill climbing. *B*: behavior of the network in *A* during a hill-climbing generalization test. Lettered dots indicate turns. Dimensions are in centimeters. The starting location is marked by an asterisk. *C*: sensory input, neuronal activation, and behavioral state probability vs. time for the behavior shown in *B*. Dashed lines indicate turns in *B*. Trace color indicates neuronal identity as shown in the key.

a–f) were restricted to intervals in which sensory input, $u(t)$, decreased rapidly. For example, at turning event *a*, the activation of *neuron 1* dropped well below that of *neuron 2*. Thus the contribution of the excitatory pathway to *neuron 3* dropped faster than the contribution of the inhibitory pathway to *neuron 3*. This difference caused *neuron 3* to desaturate, resulting in a spike in P_{turn} . Conversely, turns were absent from intervals in which sensory input dropped slowly. For example, between turning events *a* and *b*, the difference between the contribution of the excitatory and inhibitory pathway was insufficient to desaturate *neuron 3*. This motif has been identified in other optimized network models (Dunn et al. 2004; Fetzi 1993).

Sensory neuron differentiator motif

An example of this motif is shown in Fig. 4. The sensory neuron differentiator relied on a fast sensory neuron in an excitatory pathway (*neuron 0* to *neuron 3*) in parallel with a slow sensory neuron in an inhibitory pathway (*neuron 1* to *neuron 3*). The hill-climbing behavior of the network is shown in Fig. 4*B*, and the time course of neuronal activation is shown in *C*. The reduced speed of *neuron 1* was mainly attributable to the fact that its time constant was significantly greater than the time constant of *neuron 0*; a similar trend was evident in the other networks of this motif, although sometimes the roles of *neurons 0* and *1* were reversed. We noted that turning events (labeled *a–e*) were restricted to intervals in which sensory input decreased rapidly. For example, at turning event *a*, the activation of *neuron 0* increased quickly relative to the decreased activation of *neuron 1*. Thus the contribution of the excitatory pathway to *neuron 3* dropped faster than the contribution of the inhibitory pathway to *neuron 3*. This difference caused *neuron 3* to desaturate, resulting in a spike in P_{turn} . Conversely, turns were absent from intervals in which sensory input dropped slowly. For example, between turning events *d* and *e*, the difference between the contribution of the excitatory and inhibitory pathway was insufficient to desaturate *neuron 3*.

Bounce-and-trap motif

The third type of network (Fig. 5) diverged from the differentiating networks in two main respects. First, its behavior depended on absolute levels of sensory input, rather than the rate of change of sensory input. Second, this type of network had two functionally distinct pathways. One pathway was dedicated to the avoidance of regions with low levels of sensory input; we refer to this as the “bounce” pathway because the model worm appeared to bounce off a boundary where sensory input dropped below a threshold. The other pathway was dedicated to keeping the worm in regions with high levels of sensory input; we refer to this as the “trap” pathway, because the model worm was trapped at high sensory input by being forced to turn constantly.

The hill-climbing behavior of a bounce-and-trap network is shown in Fig. 5*B*, and the time course of neuronal activation is shown in *C*. At the bounce threshold (turning events *a* and *b*), the activation of *neuron 0*, the bounce pathway’s sensory neuron, decreased such that it was insufficient to keep *neuron 3* saturated (Fig. 5*C*, bottom), resulting in a spike in P_{turn} . At the target concentration (turning event *c*) *neuron 1*, the trap pathway’s sensory neuron, suddenly shifted from fully off to

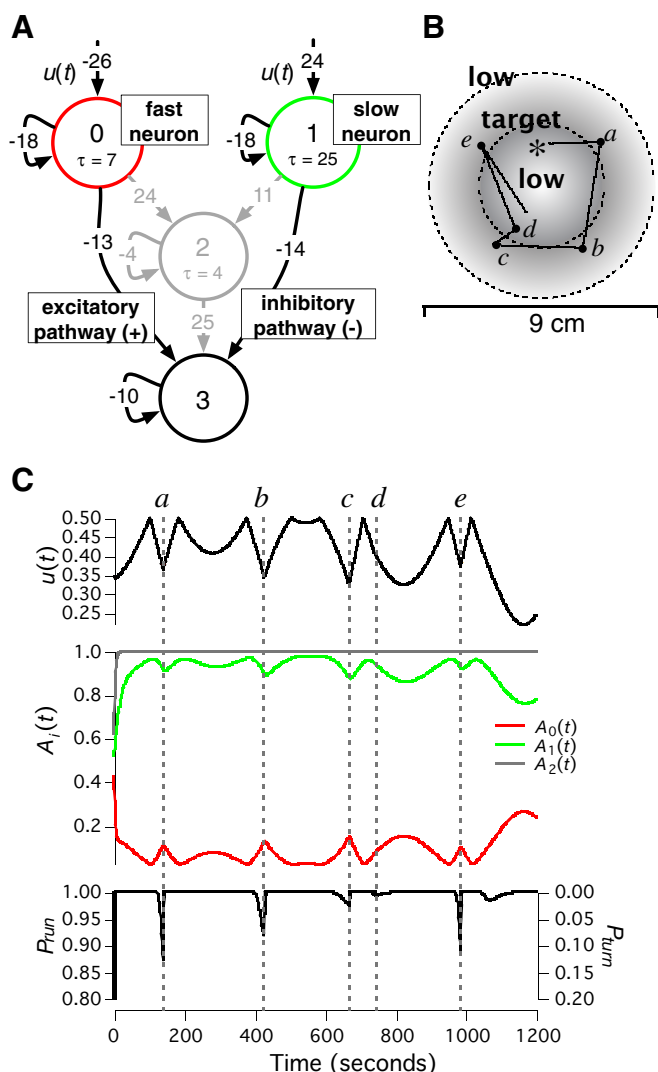


FIG. 4. Example of the sensory neuron differentiator motif. *A*: circuit diagram. Numbers associated with arrows indicate the strengths of synaptic connections or the sensory gain factor. Time constants are given in seconds. The biases of *neurons 0* and *1* were 10. *Neuron 2*, shown in gray, was excluded from the motif because its activation level was constant during hill climbing. The pathway sensory input to network output via *neuron 0* is labeled “excitatory” because it involves 2 inhibitory connections in series; the corresponding pathway via *neuron 1* is labeled “inhibitory” because there it involves one excitatory and one inhibitory connection. *B*: Behavior of the network in *A* during a hill-climbing generalization test. Lettered dots indicate turns. Dimensions are in centimeters. The starting location is marked by an asterisk. *C*: sensory input, neuronal activation, and behavioral state probability vs. time for the behavior shown in *B*. Dashed lines indicate turns in *B*. Trace color indicates neuronal identity as shown in the key.

fully on. Here, both sensory neurons were activated, but the inhibitory connection from *neuron 1* was stronger than the excitatory connection from *neuron 0*. This imbalance caused *neuron 3* to inactivate, resulting in sustained turning that tended to keep the animal at the target concentration because, over time, sustained turning reduces net translational velocity to near zero. In the network shown in Fig. 5*A*, the neuron subserving the trapping function was a sensory neuron but in other bounce-and-trap networks, the trap neuron was the interneuron; examples of such motifs appear in the goal-seeking network shown Fig. 7.

Although sustained turning is theoretically sufficient to produce trapping, it is a potentially weak trapping mechanism because of its susceptibility to occasional short runs in the down-gradient direction, which would allow the worm to escape the target region. Further analysis revealed that the efficacy of trapping was enhanced by an asymmetry built into the bounce-and-trap motif, such that it was easier to enter the target region than to leave it. Using a previously developed approach (Chiel et al. 1992), we found such an asymmetry by plotting the equilibrium points (the nullcline) of the trap sensory neuron in the A - x plane, where A is trap neuron activation and x is position in the gradient (Fig. 6). This analysis showed that for a model worm moving up the gradient, the point at which the trap neuron shifts from off to on (trapping) is much closer to the target zone than is the point at

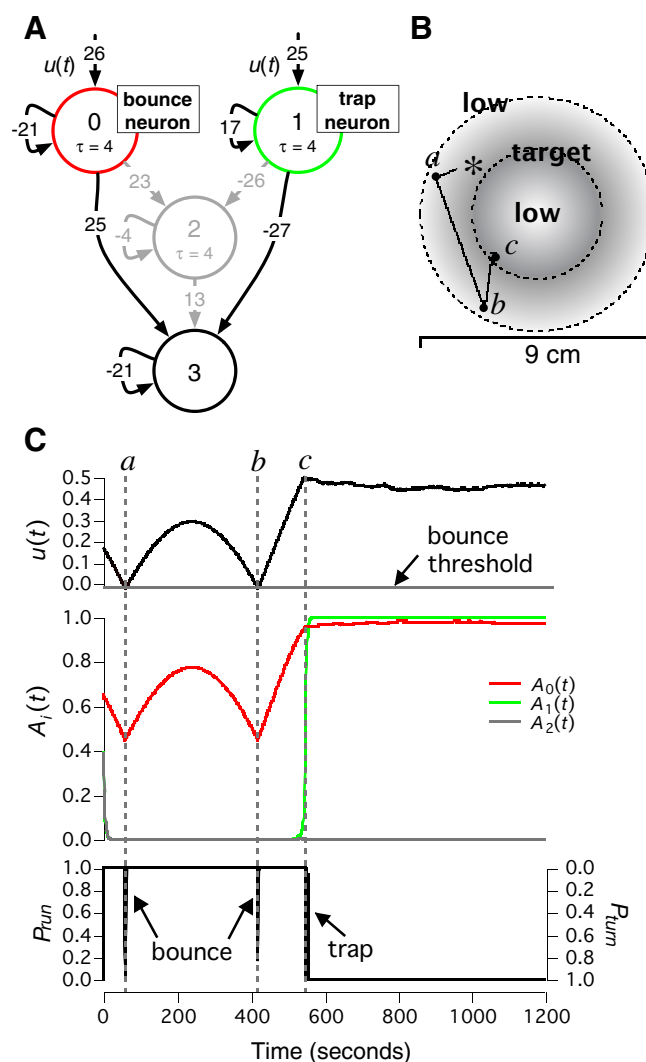


FIG. 5. Example of the bounce-and-trap motif. *A*: circuit diagram. Numbers associated with arrows indicate the strengths of synaptic connections or the sensory gain factor. Time constants are given in seconds. The biases of *neurons 0* and *1* were 10 and -15 , respectively. *Neuron 2*, shown in gray, was excluded from the motif because its activation level was constant during hill climbing. *B*: behavior of the network in *A* during a hill-climbing generalization test. Lettered dots indicate turns. Dimensions are in centimeters. The starting location is marked by an asterisk. *C*: sensory input, neuronal activation, and behavioral state probability vs. time for the behavior shown in *B*. Dashed lines indicate turns in *B*. Trace color indicates neuronal identity as shown in the key.

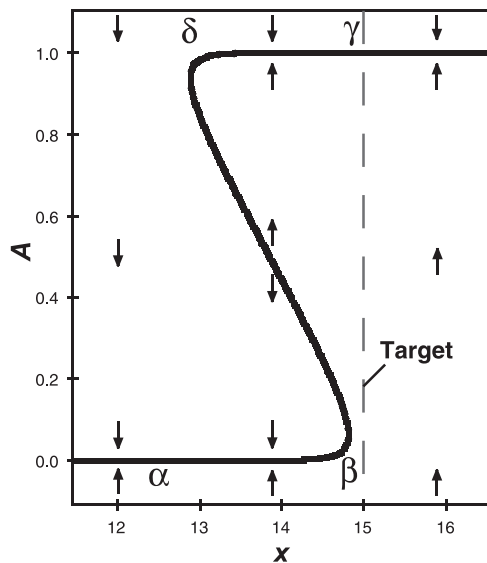


FIG. 6. Origin of the trapping behavior asymmetry. Arrows indicate the sign of $dA(t)/dt$ (up arrows, positive) indicated by Eq. 1 for the specified values of A and x . A is the instantaneous value of trap neuron activation and x defines sensory input $u(t)$ according to the linear relationship shown in Fig. 2B. The black line shows the A - x nullcline [$dA(t)/dt = 0$], which represents the equilibrium points of Eq. 1. The target concentration of 0.5 is located at the position $x = 15$ (dashed line). A worm that starts at a low concentration and moves slowly up the gradient traces the nullcline from α to β . These equilibrium points are stable because deviations from the line produce restorative values of $dA(t)/dt$. The shift from off to on (trapping, see text) takes place just to the right of β , where $dA(t)/dt$ becomes positive, driving the trap neuron to the on state. A worm that starts near the target and moves down the gradient traces another stable region of the nullcline, from γ to δ . The shift from on to off (escape, see text) takes place just to the left of δ , where $dA(t)/dt$ becomes negative, driving the trap neuron into the off state. Trapping behavior is enhanced by the fact that the escape point (δ) is further from the target zone than the trap point (β).

which, for a worm moving down the gradient, the trap neuron shifts from on to off (escape). This asymmetry can be ascribed to the strong excitatory self-connection on the trap neuron, which produces a pronounced z-shaped fold in the nullcline along the x axis; neurons with weak self-connections have no such fold (Beer 1995).

Self-connections in hill-climbing networks

Self-connections were large across all hill-climbing networks with an average absolute value of 7.4 ± 0.65 (SE), implying that such connections contributed significantly to network fitness. As noted in the preceding text, excitatory self-connections on trap neurons improved trapping behavior. Further analysis revealed two additional functions for self-connections in hill-climbing networks. First, we found that self-connections were large and inhibitory on most sensory neurons and interneurons in the differentiator networks and on all bounce neurons in bounce-and-trap networks. It has been shown that inhibitory self-connections act to reduce the effective time constant of a neuron by increasing the rate at which it relaxes to the steady state value dictated by its net input (Dunn et al. 2004). In the present study, it is likely that such connections increased network fitness by allowing neurons to respond more quickly to changes in sensory input. Second, we found that in the majority of the differentiator networks (14 of 21), the inhibitory self-connections increased the differences

between response speeds of neurons in the slow and fast pathways. It is likely that this enhancement increased fitness by making networks more sensitive to small differences in sensory input.

Goal seeking

Each goal-seeking solution was a combination of two motifs, one regulating movement in the up-gradient direction and one regulating movement in the down-gradient direction. Each component of a goal-seeking solution was analogous to one of the hill-climbing motifs described in the preceding text. The signs of synaptic connections in the up-gradient motifs matched the signs of synaptic connections in the hill-climbing motifs, as expected. In contrast, the signs of the synaptic connections in the down-gradient motifs were reversed relative to the hill-climbing sub-motifs because this motif drives movement down the gradient. The two most common goal-seeking solutions were the dual bounce-and-trap network (Table 1, $n = 31$) and the dual interneuron differentiator network (Table 1, $n = 19$). Four other combinations were rare, two were never seen, and one (Table 1, —) was formally impossible because the number of sensory neurons was limited to two.

Dual bounce-and-trap network

This type of solution was composed of two bounce-and-trap motifs, one for moving up the gradient (Fig. 7, A–C) and one for moving down the gradient (D–F). The individual bounce-and-trap motifs functioned in the same manner as the hill-climbing bounce-and-trap motif (Fig. 5) except that the trap neuron was always an interneuron instead of a sensory neuron.

Dual interneuron differentiator network

This type of solution was composed of two interneuron differentiator motifs, one for moving up the gradient (Fig. 8, A–C) and one for moving down the gradient (D–F). Individually, these motifs functioned in essentially the same manner as the hill-climbing interneuron differentiator motif (Fig. 3).

Rare networks

Three comparatively rare goal-seeking networks were also found (Table 1). The first was the bounce-and-trap/sensory neuron differentiator solution. In this type of network, the bounce-and-trap motif functioned either in the down- or up-gradient regime with the sensory neuron differentiator motif

TABLE 1. Frequencies of different types of goal-seeking networks

Up-Gradient	Down-Gradient		
	BT	SND	ID
BT	31	2	3
SND	2	—	2
ID	0	0	19

Goal-seeking networks comprised two previously identified hill climbing motifs (Figs. 3–5), one for movement up the gradient (rows) and one for movement down the gradient (columns). Frequencies are based on a sample of 59 networks. ID, interneuron differentiator; SND, sensory neuron differentiator; BT, bounce-and-trap; and —, formally impossible motif combination (see text).

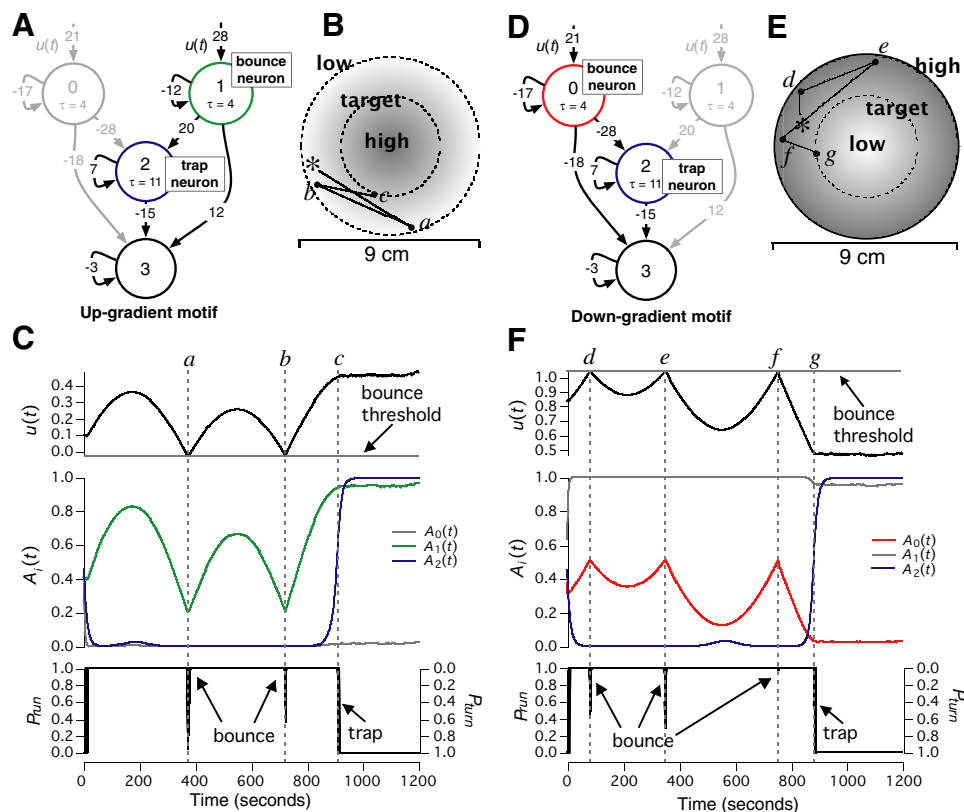


FIG. 7. Example of the dual bounce-and-trap network. **A:** circuit diagram for the up-gradient motif. Numbers associated with arrows indicate the strengths of synaptic connections or the sensory gain factor. Time constants are given in seconds. The biases of neurons 1 and 2 were 2 and -20 , respectively. Neuron 0, shown in gray, was excluded from the motif because its activation level was constant during the test. **B:** behavior of the network during a goal-seeking generalization test in which the model worm was started below the target zone. Dots indicate turns. Dimensions are in centimeters. The starting location is marked by an asterisk. **C:** sensory input, neuronal activation, and behavioral state probability vs. time for the behavior shown in **B**. Dashed lines indicate turns in **B**. Trace color indicates neuronal identity as shown in the key. **D:** circuit diagram for the down-gradient motif. The biases of neurons 0 and 2 were -13 and -20 , respectively. Neuron 1, shown in gray, was excluded from the motif because its activation level was relatively constant during the test. **E:** behavior of the network during a goal-seeking generalization test in which the model worm was started above the target zone. Symbols as in **B**. **F:** sensory input, neuronal activation, and behavioral state probability vs. time for the behavior shown in **E**. Trace color and dashed lines as in **C**.

servicing the complementary function; we obtained four such networks, two of each configuration. The second type of network was the bounce-and-trap/interneuron differentiator solution. This type was composed of an up-gradient bounce-and-

trap motif and a down-gradient interneuron differentiator motif; we obtained three such networks. The third type of network was the sensory neuron differentiator/interneuron differentiator solution. This type was composed of an up-gradient sensory

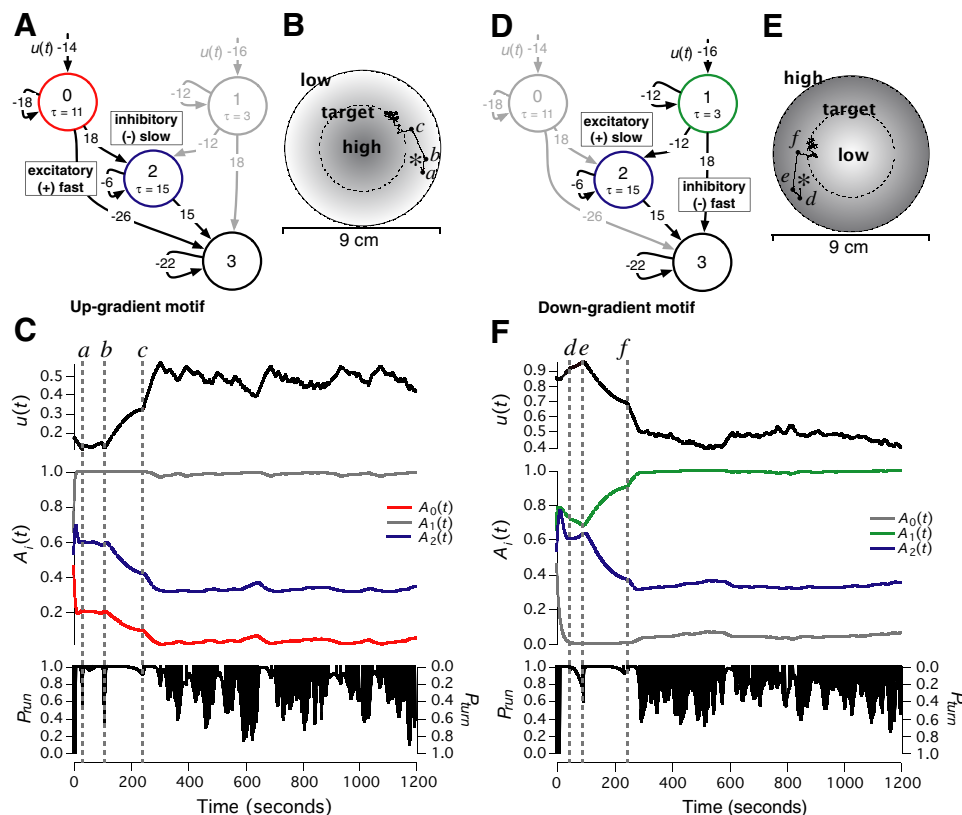


FIG. 8. Example of the dual interneuron differentiator network. **A:** circuit diagram for the up-gradient motif. Numbers associated with arrows indicate the strengths of synaptic connections or the sensory gain factor. Time constants are given in seconds. The biases of neurons 0 and 2 were 4 and 13, respectively. Neuron 1, shown in gray, was excluded from the motif because its activation level was essentially constant during the test. **B:** behavior of the network during a goal-seeking generalization test in which the model worm was started below the target zone. Dots indicate turns. Dimensions are in centimeters. The starting location is marked by an asterisk. **C:** sensory input, neuronal activation, and behavioral state probability vs. time for the behavior shown in **B**. Dashed lines indicate turns in **B**. Trace color indicates neuronal identity as shown in the key. **D:** circuit diagram for the down-gradient motif. The biases of neurons 1 and 2 were 24 and 13, respectively. Neuron 0, shown in gray, was excluded from the motif because its activation level was relatively constant during the test. **E:** behavior of the network during a goal-seeking generalization test in which the model worm was started above the target zone. Symbols as in **B**. **F:** sensory input, neuronal activation, and behavioral state probability vs. time for the behavior shown in **E**. Trace color and dashed lines as in **C**.

neuron differentiator motif and a down-gradient interneuron differentiator; we obtained two such networks. We attribute the absence of the down-gradient bounce-and-trap/up-gradient interneuron differentiator solution and the down-gradient sensory neuron differentiator/up-gradient interneuron differentiator solution mainly to sampling error. Presumably, such solutions would be found in a more exhaustive search of parameter space, although we do not exclude the possibility that parameter restrictions or interactions between up- and down-gradient parameters may make these other solutions impossible.

DISCUSSION

The main objective of the present study was to identify circuit motifs for two general classes of spatial orientation behaviors in nematodes: hill climbing and goal seeking. To do this, we used an unbiased optimization algorithm to adjust connection strengths and other parameters in small networks of generic dynamical neurons. We found three fundamental motifs: the sensory neuron differentiator, the interneuron differentiator, and the bounce-and-trap motif. Although simplified, the model retained what are likely to be essential features of sensorimotor integration in nematodes, namely a graded-processing network of sensory neurons and interneurons, and the dynamical regulation of turning frequency in a stochastic motor system. It is likely, therefore that these motifs will inform the search for the real circuits that underlie these behaviors in nematodes. More generally, the mathematical formalism used in the present study is applicable to many other types of neurons and neural circuits (Beer 2006). Thus these motifs provide possible circuits for similar tasks in other organisms.

The overall design of this study, with a consistent network architecture applied to two distinct tasks, enabled us to attribute changes in time constants, biases, and connectivity to changes in task. In the hill-climbing task, each of the three fundamental motifs was represented. Two of these motifs, the sensory neuron differentiator and the bounce-and-trap motif, appear to be novel, whereas the third motif, the interneuron differentiator, has been identified through similar means in the past (Dunn et al. 2004; Munro et al. 1994). The sensory neuron differentiator is perhaps the simplest motif in that it involves only sensory neurons and thus a single layer of processing. In the case of goal-seeking task, the networks we found were more complicated than for the hill-climbing task. Whereas a single motif was sufficient for hill climbing, each of our goal-seeking networks comprised two motifs, one dedicated to controlling behavior below the goal and one dedicated to controlling behavior above the goal. Thus our results argue that goal seeking, the more complex task at the behavioral level, is likely to be the more complex task at the level of neuronal implementation.

Previous evidence suggests that the main behavioral strategy for most forms of spatial orientation in *C. elegans* is likely to be the so-called pirouette mechanism, in which turning frequency is modulated by the time derivative of the stimulus to which the animal is orienting (Chung et al. 2006; Miller et al. 2005; Zariwala et al. 2003). The sensory neuron differentiator and interneuron differentiator motifs are consistent with this strategy in that they compute an approximate derivative of sensory inputs. The bounce-and-trap motif, however, is not

consistent with the pirouette mechanism because here turning frequency is a function of absolute concentration rather than time-dependent changes in concentration. Nevertheless, responses consistent with the bounce-and-trap motif are seen in the context of some forms of spatial orientation in *C. elegans*. For example, when encountering a patch of food, the frequency of turning events in the form of short reversals increases (Gray et al. 2005), a behavior that may contribute to trapping in the presence of food. Similarly, when encountering a region of high osmolarity (500 mM), a nematode performs a large turn known as an avoidance response (Culotti and Russell 1978), a behavior that is similar to the bounce component of the bounce-and-trap mechanism. The overall correspondence between behavioral strategies believed to exist in *C. elegans* and the functionality of the motifs described here justifies attention to them as possible circuit modules.

Thermotaxis is the best understood example of goal-seeking behavior in *C. elegans*, yet the behavioral mechanism underlying thermotaxis remains unclear. At temperatures above the goal, migration is believed to involve a biased random walk via the pirouette mechanism (Chung et al. 2006; Ryu and Samuel 2002; Zariwala et al. 2003). At temperatures below the goal, however, some studies have consistently found evidence only for an unbiased random walk (Chung et al. 2006; Ryu and Samuel 2002; but see Ito et al. 2006; Zariwala et al. 2003), raising the question of how goal-seeking behavior is nevertheless achieved.

One possible answer is provided by the up-gradient bounce-and-trap/down-gradient interneuron differentiator networks obtained in the goal-seeking task. In these networks, when the model worm is below the goal, the bounce-and-trap mechanism is utilized such that migration occurs by random locomotion coupled with bouncing at the gradient margin and trapping (via persistent turning) near the goal. We propose that during thermotaxis in real worms, up-gradient migration could be achieved in a similar way. The role of the bounce component of the bounce-and-trap mechanism is fulfilled mainly by repulsion from the dry margins of the assay plate. The role of the trap component is fulfilled by either of two previously documented responses exhibited at the preferred temperature: pirouettes when moving in either direction away from the temperature goal (Zariwala et al. 2003) or isothermal tracking (Hedgecock and Russell 1975) in which the worm closely follows a linear trajectory orthogonal to the gradient (Luo et al. 2006; Mori and Ohshima 1995). Thus the present study provides an existence proof for a behavioral mechanism for thermophilic migration in the absence of a pirouette mechanism.

For simplicity of exposition, nodes in the model networks describe here were presented as neurons, but at least three other types of relationship between nodes and biological entities are conceivable. First, a node can represent a group of co-active neurons. For example, here we found that a single sensory neuron is sufficient for hill-climbing behavior, whereas hill climbing in real nematodes seems to require multiple sensory neurons, at least in the case of chemotaxis and aerotaxis (Bargmann and Horvitz 1991; Chang et al. 2006; Rogers et al. 2006). If it is found that in a real network certain groups of sensory neurons are co-active, they could be combined into a single entity when the network is compared with the motifs we have described. Similar arguments can be made in regard to the

multiple sensory neurons involved in aerotaxis (Chang et al. 2006; Rogers et al. 2006) or the many interneurons that are downstream of sensory neurons in chemotaxis and thermotaxis (Gray et al. 2005; Mori and Ohshima 1995; Tsalik and Hobert 2003). Second, a node can represent a step in a subcellular signaling pathway within a neuron. This representation is appropriate because subcellular signaling pathways are usually modeled in terms of the concentration of intracellular messengers in various cellular compartments and the differential equations representing these concentrations have essentially the same form as the equations used here to represent neuronal activations (Smolen et al. 2001; Sontag et al. 2004). Third, the motifs presented here can be interpreted as dynamical systems that capture in compressed form the essential features of the dynamics of the real system understood as the set of all neurons necessary for hill-climbing and goal-seeking behaviors in *C. elegans*. This interpretation follows from previous demonstrations that dynamical neural networks such as those defined by Eqs. 1 and 2 are universal approximators of smooth dynamics (Chow and Li 2000; Funahashi and Nakamura 1993; Kimura and Nakano 1998). In the present instance, the dynamics to be approximated are the space-time trajectories of real worms during chemotaxis, thermotaxis, aerotaxis, etc.

Although the extent to which the neural computations underlying spatial orientation in *C. elegans* are carried out at the subcellular versus the network level remains unclear, precedents exist for the computation of sensory derivatives at both levels in other organisms. Subcellular computation of derivatives has been demonstrated in the case of chemotaxis behavior in single-celled organisms such as bacteria and paramecia (Block et al. 1982; Machemer 1989; Wadhams and Armitage 2004). Network-level computation of derivatives has been demonstrated in the case of contrast and motion detection in the visual system (Clifford and Ibbotson 2002; Dowling and Werblin 1969; Werblin and Dowling 1969). The set of motifs described here serve as working hypotheses for computations at either level in *C. elegans*.

ACKNOWLEDGMENTS

We are grateful to D. Pate for technical assistance and S. Faumont for comments.

GRANTS

This work was supported by National Science Foundation Grants IOS-0080068 and IOS-0543643.

REFERENCES

- Bargmann C, Horvitz H.** Chemosensory neurons with overlapping functions direct chemotaxis to multiple chemicals in *C. elegans*. *Neuron* 7: 729–742, 1991.
- Beer R.** On the dynamics of small continuous-time recurrent neural networks. *Adapt Behav* 3: 469–509, 1995.
- Beer R.** Parameter space structure of continuous-time recurrent neural networks. *Neural Comp* 18: 3009–3051, 2006.
- Block S, Segall J, Berg H.** Impulse responses in bacterial chemotaxis. *Cell* 31: 516–526, 1982.
- Chalfie M, Sulston J, White J, Southgate E, Thomson J, Brenner S.** The neural circuit for touch sensitivity in *C. elegans*. *J Neurosci* 5: 956–964, 1985.
- Chang A, Chronis N, Karow D, Marletta M, Bargmann C.** A distributed chemosensory circuit for oxygen preference in *C. elegans*. *PLoS Biol* 4: e274, 2006.
- Cheung B, Cohen M, Rogers C, Albayram O, de Bono M.** Experience-dependent modulation of *C. elegans* behavior by ambient oxygen. *Cur Biol* 15: 905–917, 2005.
- Chiel HJ, Beer RD, Gallagher JC.** Evolution and analysis of model CPGs for walking. I. Dynamical modules. *J Comput Neurosci* 7: 99–118, 1999.
- Chow TWS, Li XD.** Modeling of continuous time dynamical systems with input by recurrent neural networks. *IEEE Trans Circuits Syst Fund Theory Appl* 47: 575–578, 2000.
- Chung SH, Clark DA, Gabel CV, Mazur E, Samuel AD.** The role of the AFD neuron in *C. elegans* thermotaxis analyzed using femtosecond laser ablation. *BMC Neurosci* 7:30, 2006.
- Clifford CWG, Ibbotson MR.** Fundamental mechanisms of visual motion detection: models, cells and functions. *Prog Neurobiol* 68: 409–437, 2002.
- Culotti J, Russell R.** Osmotic avoidance defective mutants of the nematode *C. elegans*. *Genetics* 90: 243–256, 1978.
- Davis RE, Stretton AOW.** Signaling properties of *Ascaris* motoneurons: graded active response, graded synaptic transmission, and tonic transmitter release. *J Neurosci* 9: 415–425, 1989.
- Dowling JE, Werblin FS.** Organization of retina of the mudpuppy, *Necturus maculosus*. I. Synaptic structure. *J Neurophysiol* 32: 315–338, 1969.
- Dunn NA, Conery JS, Pierce-Shimomura JT, Lockery SR.** A neural network model of chemotaxis predicts functions of synaptic connections in the nematode *C. elegans*. *J Comput Neurosci* 17: 137–147, 2004.
- Dusenbery D.** Responses of the nematode *C. elegans* to controlled chemical stimulation. *J Comp Physiol* 136: 127–331, 1980.
- Fetz E.** Dynamic neural network models of sensorimotor behavior. In: *The Neurobiology of Neural Networks*, edited by Gardner D. Cambridge, MA: MIT Press, 1993, p. 165–190.
- Funahashi K, Nakamura Y.** Approximation of dynamical systems by continuous time recurrent neural networks. *Neural Networks* 6: 801–806, 1993.
- Goodman M, Hall D, Avery L, Lockery S.** Active currents regulate sensitivity and dynamic range in *C. elegans* neurons. *Neuron* 20: 763–772, 1998.
- Gray JM, Hill JJ, Bargmann CI.** Inaugural article: a circuit for navigation in *C. elegans*. *Proc Natl Acad Sci USA* 102: 3184–3191, 2005.
- Gray J, Karow D, Lu H, Chang A, Chang J, Ellis R, Marletta M, Bargmann C.** Oxygen sensation and social feeding mediated by a *C. elegans* guanylate cyclase homologue. *Nature* 430: 317–322, 2004.
- Hedgecock E, Russell R.** Normal and mutant thermotaxis in the nematode *C. elegans*. *Proc Natl Acad Sci USA* 72: 4061–4065, 1975.
- Hopfield JJ.** Neural networks and physical systems with emergent collective computational abilities. *Proc Natl Acad Sci USA* 79: 2554–2258, 1982.
- Ito H, Inada H, Mori I.** Quantitative analysis of thermotaxis in the nematode *C. elegans*. *J Neurosci Methods* 154: 45–52, 2006.
- Kimura M, Nakano R.** Learning dynamical systems by recurrent neural networks from orbits. *Neural Networks* 11: 1589–1599, 1998.
- Luo L, Clark D, Biron D, Mahadevan L, Samuel A.** Sensorimotor control during isothermal tracking in *C. elegans*. *J Exp Biol*, 209: 4652–4662, 2006.
- Machemer H.** Cellular behaviour modulated by ions: Electrophysiological implications. *J Protozool* 36: 463–487, 1989.
- Masters T.** *Practical Neural Network Recipes in C++*. New York: Morgan Kaufmann, 1993.
- Miller A, Thiele T, Faumont S, Moravec M, Lockery S.** Step-response analysis of chemotaxis in *C. elegans*. *J Neurosci* 25: 3369–3378, 2005.
- Milo R, Shen-Orr S, Itzkovitz S, Kashtan N, Chklovskii D, Alon U.** Network motifs: simple building blocks of complex networks. *Science*, 298: 824–827, 2002.
- Mori I, Ohshima Y.** Neural regulation of thermotaxis in *C. elegans*. *Nature* 376: 344–348, 1995.
- Munro E, Shupe L, Fetz E.** Integration and differentiation in dynamical recurrent neural networks. *Neural Comput* 6: 405–419, 1994.
- Pierce-Shimomura J, Morse T, Lockery S.** The fundamental role of pirouettes in *C. elegans* chemotaxis. *J Neurosci* 19: 9557–9569, 1999.
- Press W, Teukolsky S, Vetterling W, Flannery B.** *Numerical Recipes in C* (2nd ed.). New York: Cambridge, 1992.
- Rogers C, Persson A, Cheung B, de Bono M.** Behavioral motifs and neural pathways coordinating O₂ responses and aggregation in *C. elegans*. *Curr Bio* 16: 649–659, 2006.
- Ryu WS, Samuel AD.** Thermotaxis in *C. elegans* analyzed by measuring responses to defined thermal stimuli. *J Neurosci* 22: 5727–5733, 2002.
- Sambongi Y, Nagae T, Liu Y, Yoshimizu T, Takeda K, Wada Y, Futai M.** Sensing of cadmium and copper ions by externally exposed ADL, ASE, and ASH neurons elicits avoidance response in *C. elegans*. *Neuroreport* 10: 753–757, 1999.

- Smolen P, Baxter D, Byrne J.** Modeling circadian oscillations with interlocking positive and negative feedback loops. *J Neurosci* 21: 6644–6656, 2001.
- Sontag E, Kiyatkin A, Kholodenko B.** Inferring dynamic architecture of cellular networks using time series of gene expression, protein and metabolite data. *Bioinformatics* 20: 1877–1886, 2004.
- Suzuki H, Kerr R, Bianchi L, Jensen C, Slone D, Xue J, Gerstbrein B, Driscoll M, Schafer W.** In vivo imaging of *C. elegans* mechanosensory neurons demonstrates a specific role for the mec-4 channel in the process of gentle touch sensation. *Neuron* 39: 1005–1017, 2003.
- Tsalik L, Hobert O.** Functional mapping of neurons that control locomotory behavior in *C. elegans*. *J Neurobiol* 56: 178–197, 2003.
- Wadhams GH, Armitage JP.** Making sense of it all: Bacterial chemotaxis. *Nat Rev Mol Cell Biol* 5: 1024–1037, 2004.
- Ward S.** Chemotaxis by the nematode *C. elegans*: identification of attractants and analysis of the response by use of mutants. *Proc Natl Acad Sci USA* 70: 817–821, 1973.
- Ward S.** Nematode chemotaxis and chemoreceptors. In: *Taxis and Behavior*, edited by Hazelbauer G. London: Chapman and Hall, 1978, p. 141–168.
- Ward S, Thomson N, White JG, Brenner S.** Electron microscopical reconstruction of the anterior sensory anatomy of the nematode *C. elegans*. *J Comp Neurol* 160: 313–338, 1975.
- Werblin FS, Dowling JE.** Organization of the retina of the mudpuppy, *Necturus maculosus*. II. Intracellular recording. *J Neurophysiol* 32: 339–355, 1969.
- White JG, Southgate E, Thomson JN, Brenner S.** The structure of the nervous system of the nematode *C. elegans*. *Philos Trans R Soc Lond B Biol Sci*, 314: 1–340, 1986.
- Zariwala Z, Miller A, Faumont S, Lockery S.** Step response analysis of thermotaxis in *C. elegans*. *J Neurosci* 23: 4369–4377, 2003.
- Zheng Y, Brockie PJ, Mellem JE, Madsen DM, Maricq AV.** Neuronal control of locomotion in *C. elegans* is modified by a dominant mutation in the glr-1 ionotropic glutamate receptor. *Neuron* 24: 347–361, 1999.